Available online at www.CivileJournal.org

Civil Engineering Journal

(E-ISSN: 2476-3055; ISSN: 2676-6957)

Vol. 11, No. 08, August, 2025

Experimental Assessment of Ground Thermal Properties for Shallow Geothermal Energy

Mahmoud Irshidat [1], Sufian Qaiymah [1], Wassel Al-Bodour [1*]

[1] *Department of Civil Engineering, The University of Jordan, Amman 11942, Jordan.*

Received 06 December 2024; Revised 13 June 2025; Accepted 02 July 2025; Published 01 August 2025

Abstract

Geothermal energy, being clean and renewable on both large and small scales, has become a field of interest for researchers in several areas such as cooling-heating systems, geothermal piles, and geothermal electricity. The purpose of this study is to explore the ground thermal behavior and relevant thermal soil properties for key regions in Jordan. These regions represent either major cities or areas with optimal seasonal temperature variations suitable for such applications. Three key locations were investigated: Tabarbour-Amman, Shafa-Badran-Amman, and Mafraq. Geotechnical soil investigations were conducted using hollow stem auger drilling, with soil samples collected at each meter of depth. Each sample was tested in the laboratory for thermal diffusivity, heat capacity, specific heat, and thermal conductivity. Additionally, thermocouples were installed in each borehole, and the holes were backfilled with the soil cuttings produced during drilling. Seasonal temperature profiles were developed for each site based on the measurements from the thermocouples. Temperature variations were also analyzed using the measured thermal soil properties within a mathematical heat transfer model, with results showing good agreement with the recorded measurements. Thermal diffusivity ranged from 0.315 to 0.365 mm²/s near the ground surface, and from 0.135 to 0.257 mm²/s at a depth of six meters. Thermal conductivity ranged from 0.197 to 0.351 W/m·K near the surface to 0.468 to 0.875 W/m·K at six meters depth. Ground temperature varied from a maximum during the hot season at the surface to a minimum during the cold season at six meters depth. The extreme temperature difference (4.4 to 5.25 °C), along with the observed values of diffusivity and heat capacity, indicates significant potential for energy extraction in the form of heat, in a cost-effective and time-efficient manner.

Keywords: Geothermal Energy; Soil; Thermal Diffusivity; Thermal Conductivity; Heat Capacity; Heat Storage.

1. Introduction

This study aims to assess the thermal characteristics of soil at three strategic locations in Jordan, focusing on the soil's capacity to release or absorb heat from the earth. In general, the temperature remains nearly constant within the upper 100 meters of the Earth's crust, increasing slightly with depth at a rate of approximately +2.5 °C per 100 meters. This makes the subsurface environment suitable for geothermal exchange systems. In addition to the temperature gradient, the thermal properties of the geo-column also influence the efficiency of energy extraction or ejection to the earth [1]. Key factors that govern geothermal heat exchange include the soil temperature at the collector depth, ground thermal diffusivity, thermal conductivity, heat capacity, and specific heat. One significant parameter that indicates the ground's capacity for heat storage is thermal diffusivity (α). Diffusivity varies considerably with depth (pressure), soil specific gravity (mineral composition), moisture content, and soil structure (void ratio) [2].

* Corresponding author: w.bodour@ju.edu.jo

http://dx.doi.org/10.28991/CEJ-2025-011-08-013

This study investigates the thermal potential and characteristics of various soils based on experimental measurements conducted on samples collected from three different sites in Jordan, where the ground temperature profile was also monitored. Field exploration, in-situ measurements, and a laboratory testing program were carried out to achieve the study's objectives. Due to the lack of sufficient information and prior studies on the thermal properties of soil and rock in the region, it is challenging to draw reliable conclusions regarding the potential for geothermal energy in Jordan. As a result, the use of ground energy extraction and injection technologies remains uncommon in the country. A few projects have been attempted, but they failed to deliver satisfactory results due to insufficient characterization of subsurface conditions for their intended applications [3].

Heat transport within soil occurs primarily through conduction, with smaller contributions from convection and radiation; particularly under extremely dry or high-temperature conditions [4]. Water content is another key factor influencing soil heat exchange, affecting temperature and heat flux over time and depth within specific ranges [5]. Both specific heat and volumetric heat capacity increase with moisture content and soil density. Clay generally exhibits higher values than sandy soil due to its greater water-holding capacity [6]. Soil moisture content significantly influences ground temperature, primarily by affecting thermal conductivity within a limited depth (up to 10 m). Thermal conductivity shows considerable variation in very dry soils but only minor changes in wet soils [7]. Thermal diffusivity, which also impacts ground temperature, is typically estimated at 0.05 m^2/day or lower under stable conditions. High thermal diffusivity increases the ground's susceptibility to temperature fluctuations caused by external sources, though its seasonal variations are often negligible ([5, 6]). On the other hand, .García-Noval et al. [8] studied the thermal properties for some regions in Spain, the found some relations between the rock mineralogy, structure, and age with thermal conductivity.

On the other hand, considering environmental and economic impacts along with the efficiency of power-producing systems, a 3D heat transfer model of shallow, low-temperature Aquifer Thermal Energy Storage (ATES) systems for space heating and cooling was developed to evaluate power densities for different ATES setups in gravel. Though the power density was limited to 3.2 W/m^2, it reduced heating-related emissions by up to 70,000 tons of CO_2 annually and met 92% of the residential heating demand [9]. Moreover, since commercial buildings account for 37% of global CO_2 emissions, geothermal energy offers an economic, environmental, and sustainable heating solution, making it a strong competitor to fossil fuels for commercial heating [10]. Ground-source heat pump (GSHP) systems have also been found to be more energy-efficient than traditional air-source air conditioning (ASAC) systems [11]. The energy consumed by heat pumps is as low as two-thirds of the energy they produce, in addition to significantly reducing greenhouse gas emissions [12].

Based on the above, and in light of the current economic and environmental conditions, geothermal energy has become a national priority for the Ministry of Energy and Mineral Resources. Additionally, it has been designated a national priority by Jordan's highest research council, the Scientific Research Fund. The use of geothermal energy in Jordan is still in its early stages—for example, at the American University of Madaba and in some residential buildings—and further investigation is needed due to a lack of geo-data and information. (IRENA 202)-Jordan [3].

This study was established to lay the groundwork for future geothermal research and projects aimed at developing clean and renewable energy solutions in Jordan. As the concept is still in its early stages, the primary objective of the study is to assess the potential for utilizing geothermal energy by testing the thermal properties of the ground. The results are then compared to typical values observed in similar geological formations in other countries. Key parameters such as thermal diffusivity, conductivity, capacity, and specific heat were tested and evaluated across various sites. Additionally, the study implemented an instrumentation system designed to monitor the temperature profile with depth. Four field stations were established for these measurements and soil analysis.

The testing sites represent four key locations in Jordan: Irbid, Al-Mafraq, Amman-Tabarbour, and Amman-Shafa Badran. Amman, the capital and most populous city in Jordan, includes the districts of Tabarbour and Shafa Badran, which feature silty and clay soils, respectively. These soil types are commonly found across other areas of Amman as well. Regardless of location, limestone serves as the predominant bedrock throughout all regions of Amman. In contrast, the soils of Irbid and Al-Mafraq are notably distinct from those in other parts of the country. Irbid's clay soils are characterized by a Mediterranean red hue, resulting from the weathering of local rock. Al-Mafraq, on the other hand, is primarily composed of yellow clays. Irbid is Jordan's second-largest city and the largest in the northern region, while Al-Mafraq is considered the central city of Jordan's northern desert. The locations of the study sites are shown in Figure 1.

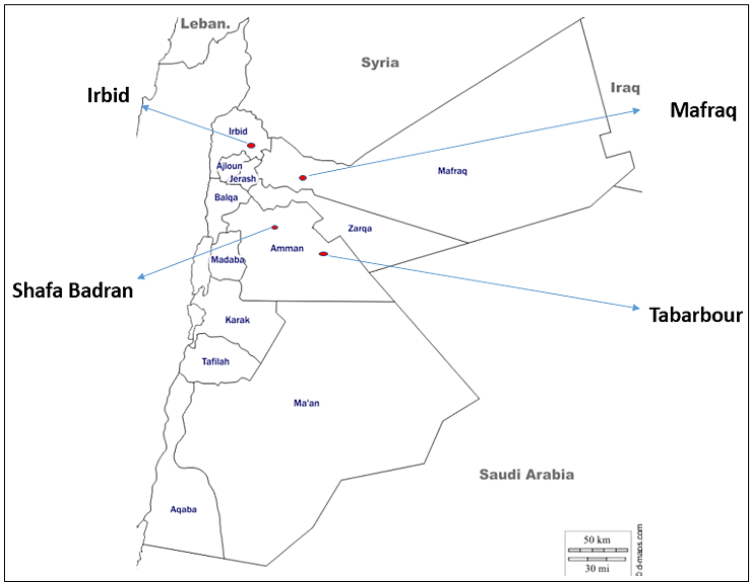

Figure 1. The exact location of sample

2. Framework

This study was conducted by combining field measurements, experimental tests, mathematical analysis, and data collection to characterize and validate the thermal behavior, temperature variations, and thermal parameters of soil. Soil samples were collected at depths ranging from near the ground surface to six meters deep, from four boreholes drilled at three different sites. The sampling frequency was one sample per meter of borehole depth. After drilling and sampling, thermocouples were installed at the Tabarbour site. Six temperature sensors were placed at one-meter vertical intervals to monitor seasonal and daily variations in the temperature profile. For study validation purposes, temperature variations were also analyzed using a mathematical model, with input parameters obtained from the thermal soil properties interpreted from laboratory testing and measurements. The mathematical model requires that the boundary conditions be known in order to solve the model.

The assumption that the surface temperature—over a relatively large area near the test points—is uniform during a specific time period reduces the problem to a one-dimensional form, with a surface boundary condition that sets the temperature equal to the climate temperature averaged over the selected period. A seasonal mean temperature value is used, since seasonal variation in the selected location is relatively significant. Temperature data were collected from the nearest measurement stations and are publicly available on the website of the Jordan Meteorological Department (*https://www.accuweather.com/ar/jo/amman/221790/january-weather/221790*).

Accordingly, the temperature data were optimally categorized based on the least variation over specific periods of the year (2022). This was achieved by plotting temperature variations over time throughout the year. From the resulting curves, time windows with the minimum possible variation were identified (Figures 2 to 5). Four distinct periods were recognized: Winter (beginning December 21st), Spring (beginning March 21st), Summer (beginning June 21st), and Autumn (beginning September 21st).

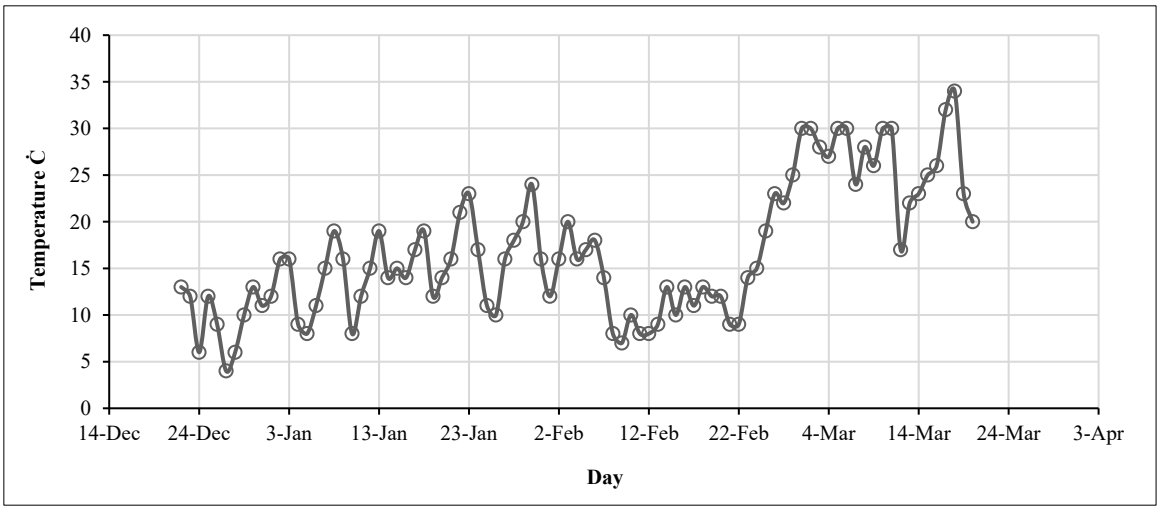

Figure 2. Winter temperature variations of 2022

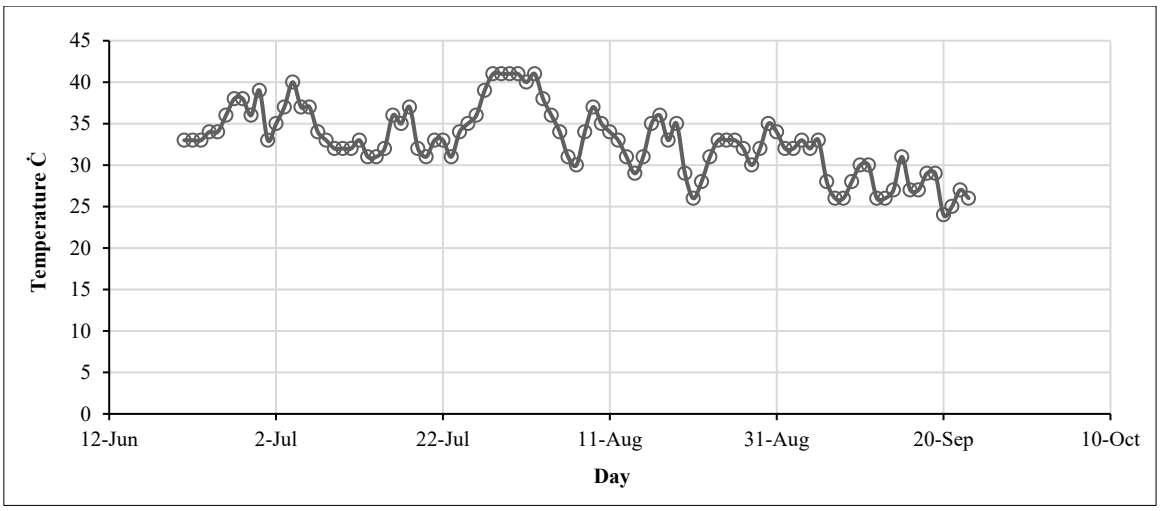

Figure 3. Summer temperature variation of 2022

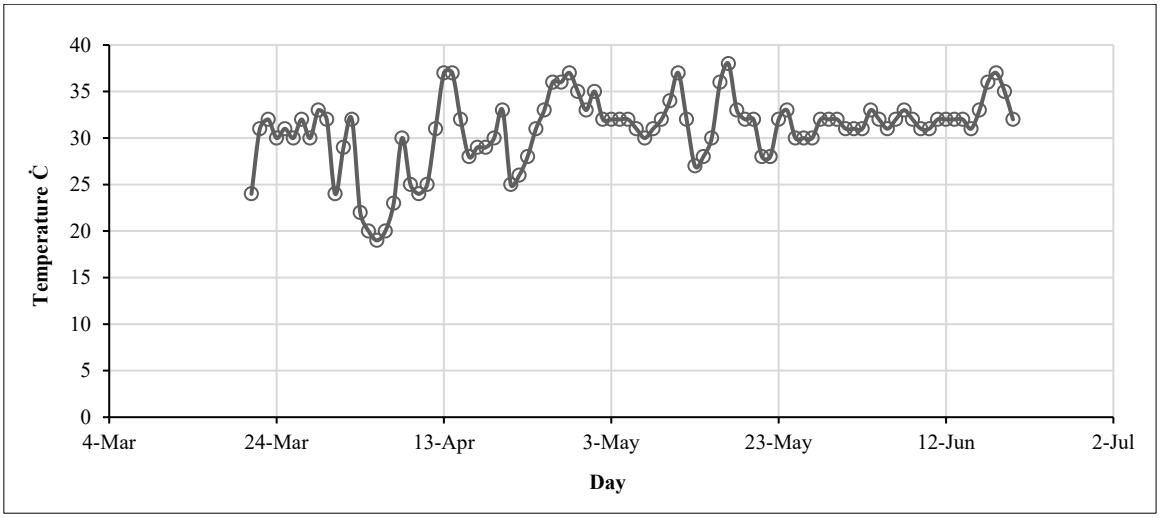

Figure 4. spring temperature var of 2022

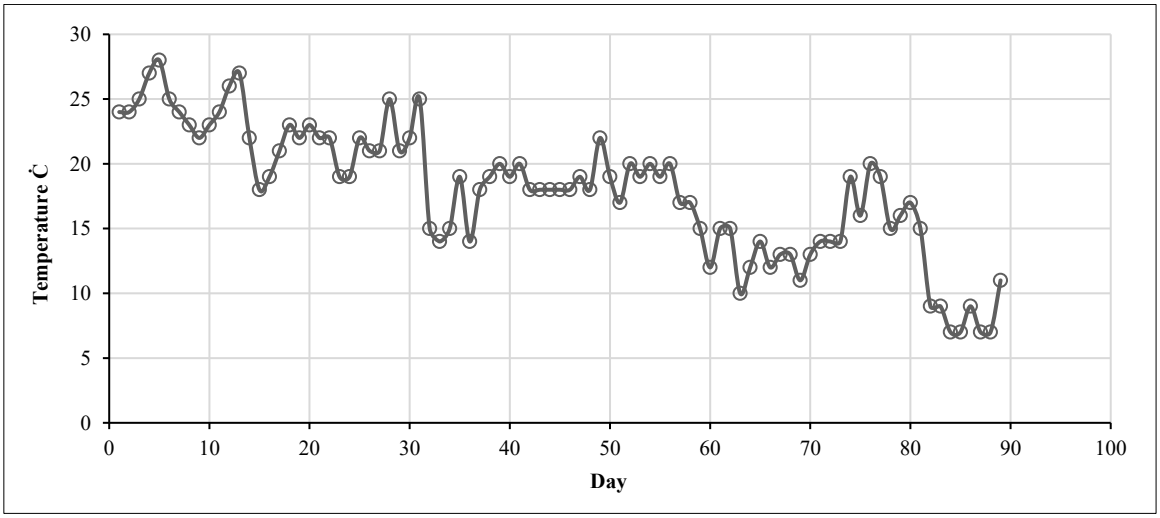

Figure 5. Autom temperature variations of 2022

The temperature was averaged for each of the designated time periods. Then, the mathematical model was solved using the interpreted and/or measured thermal properties of the soil, along with the measured surface temperature for each averaged period. Finally, the results of the mathematical model for the temperature profile with soil depth, based on the given surface temperature, were validated and compared with the temperature profiles obtained from field measurements using thermocouples.

3. Theoretical Premise

The concept of using geothermal heat from the upper shallow portion of the Earth's crust is primarily limited to heat exchange applications. The most common approach involves circulating a fluid (such as air) through the ground. In winter, while the air temperature can drop below zero degrees Celsius, the ground temperature remains relatively constant at around 12 to 14 °C. Circulating the cold fluid through the ground for a sufficient amount of time raises its temperature to a level close to that of the ground. The heat gained in this process can be used for various purposes, such as residential heating systems. In summer, the process can be reversed to provide cooling.

Several researchers have investigated differences in soil temperature at various depths [13, 14]. Near the surface, monthly average soil temperatures are known to follow a simple harmonic function over typical annual cycles. As a result, the following equation can be solved and used to analyze soil temperature based on known surface temperatures [15], allowing comparison with measured values. Heat transfer is assumed to follow the one-dimensional Fourier law of heat conduction.

$$d^2Tdx^2 = \frac{1}{\alpha} \times \frac{dT}{dt} \quad (1)$$

where T is temperature, α is the thermal diffusivity, x: is the distance, t is the time.

In this context, the soil or rock stratum is idealized as a line in the direction of x (depth), assuming one-dimensional heat transfer due to uniformity and infinite lateral extent. One end of this line represents a known boundary—the surface temperature—while the other end extends to an unknown depth where heat transfer stabilizes at its natural equilibrium. This stable temperature depth is known as the depth of influence and can be determined using mathematical models or field measurements.

Variable heat fluxes occur regularly due to both daily and annual surface temperature cycles. Given that convection, solar radiation, and evaporative heat fluxes make negligible contributions to heat transfer in this application, the surface boundary condition of the ground can be set as:

$$at\ x = x_{inf} \quad \frac{dT}{dx} = 0 \quad (2)$$

where x_{inf} is the depth of influence after which the ground's temperature becomes independent of the surface temperature.

The solution to the heat transfer Equation 1 with this boundary conditions (for $x = 0$: Ts = f(t), and for $x_{inf} \rightarrow \infty$: T → Ts), is provide by Carslow et al. [16] as

$$T_s = T_m - T_p \cos(W.t - Q) \quad (2)$$

where T_s is the soil temperature at any depth x, T_m is the annual average temperature of soil in the stable layer; it is commonly set to the average temperature of air, practically the average temperature in the place (°C), T_p is the amplitude (C°); $= T_{max} - T_{min}$, W is the angular frequency (rad/s). The rate of change of the function argument in units of radians per second; W is $(2\pi\ /\ T)$, T is the period of the sinusoid; in this case the annual temperature cycle, T = 365.24×24×3600 =3.1557×10^7 s, and Q is Phase (rad).

Starting time (t = 0) is set to begin from January 1st of the year. This method of measuring time naturally results in a phase shift, as the beginning of the sinusoid generally does not coincide with t = 0. The subsurface is treated as a semi-infinite domain, d= {at X(x,y,z): (-∞ < x,y <∞, 0 ≤ z <∞)} The subsurface temperature T(z,t), at any point (z) and time (t) using the heat conduction equation. The soil temperature profile as a function of depth is established by solving the transient-state heat equation for a semi-infinite domain, with the surface temperature constrained by Equation 2 [16]. The temperature of the ground at any depth z can then be obtained from Equation 3:

$$T_s(z,t) = T_m - T_p \exp\left(-z^2\sqrt{\frac{w}{2\alpha}}\right) \cos\left(wt - Q - z^2\sqrt{\frac{w}{2\alpha}}\right) \quad (3)$$

Z is the depth in meter.

Equation 3 highlights the key characteristics of soil temperature evolution with depth, down to 10 meters. The second term in the equation approaches zero as depth increases, which leads to an intensified phase shift and an exponential decay in temperature amplitude. This indicates that soil temperature tends to stabilize around a constant value in the ground equilibrium zone.

4. Subsurface Exploration and Field Measurements

A subsurface exploration program was designed to support this work by collecting soil samples for a laboratory testing program, through which soil parameters can be measured directly or interpreted indirectly from test results. The Hollow Stem Auger method was used for soil drilling and sampling, offering the advantage of easier field installations. This method facilitates the recovery of samples from various depths with differing levels of quality. The outside diameter of the auger is 5 inches (12.5 cm), resulting in a borehole diameter of 5.5 inches (14 cm). Samples were collected at regular one-meter depth intervals. Thin-wall tube (Shelby tube) and split soon samples were used for soils, while double-core samples were used for rock coring. Four locations were explored, with a single borehole drilled at each site. The drilling depth was six meters at all sites. The upper portion of each borehole consisted of soil, while the lower portion consisted of rock. The locations and borehole details are presented in Table 1.

Table 1. Boreholes locations and geologic formations

No.	Borehole No.	Location	Depth (m)	Soil depth and description	Rock depth and description
1	BH-1	Shafa Badran	6	5 m (sand)	5-6m: limestone
2	BH-2	Mafraq	6	5 m (clay)	5-6m: limestone
3	BH-3	Tabarbour	6	5 m (silt)	5-6m: limestone
4	BH-4	Irbid	6	5 m (clay)	Primarily Basalt

Six samples were collected from each site. Split barrel samples were collected in glass jars, and undisturbed soil samples were collected in thin-walled tubes. This procedure was strictly followed to maintain the samples' field conditions. The samples were labeled with the required information and transported to the laboratory. After the drilling was completed, thermocouples were installed in the borehole, which was refilled with soil cuttings produced by the drilling operations. This ensured that the soil temperature detected by the sensors was accurate. Temperature variations were monitored on-site, and readings were recorded every six minutes by the temperature sensor. The sensor's information and specifications are provided in Table 2, and the sensor is shown in Figure 6.

Table 2. Thermo-Sensor specifications

Product Name	Resistance Sensor Theory Temperature Sensor 5K 12K 30K ohm Beta 3950 3435 NTC Thermistor
Element	PT100 PT1000 CLASS A/B, NTC
Housing	SUS304/ SUS316/ Brass/ ABS, can be customized
Wire Length	1 meter/ 2 meters, can be customized
End	Bare end or connectors (JST, MOLEX, TE and etc.)
Working Temp.	-50~600C, can be customize as per customer's request
Application	Home appliance, industrial equipment, auto , HVAC, and etc.
Product Name	Resistance Sensor Theory Temperature Sensor 5K 12K 30K ohm Beta 3950 3435 NTC Thermistor

Figure 6. Temperature thermocouple sensor

To calibrate the thermocouples and ensure that the sensors were reading temperature and voltage within permissible limits, a simple comparison method was used. Two soil block samples, with densities similar to those found in the field, were prepared. One soil block was dry, and the other was wet. The temperature of the samples was varied several times: by heating directly in an oven for the dry sample, and by heating water for the wet sample. The temperature of the blocks was measured using a thermometer and a laboratory soil thermometer (304 stainless steel, with a measurement accuracy

of 0.1°C). Temperature was measured over a range of 5 to 35°C, and the tolerance in readings between the two instruments was within 0.1°C.

The installation configuration and arrangement of the thermocouple are shown in the schematic diagram in Figure 7, with field photos provided in Figure 8. These photos illustrate the temperature sensor installation steps in the borehole, where PVC pipes are used to hold the sensors with adhesive materials. A scene of the drilling and sampling process is shown in Figures 9 and 10.

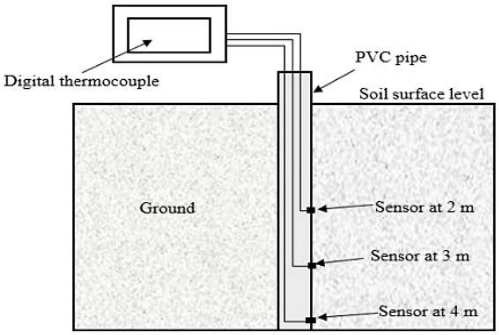

Figure 7. Schematic diagram for temperature sensors installation

Figure 8. PVC pipe used for sensors installation

Figure 9. Drilling and sampling (Al-Mafraq)

Figure 10. Soil sampling (Tabarbour)

A field experiment was carried out at Tabarbour, Amman, from March 4 to March 15, 2022. Temperatures in the Earth at different depths of 0, 1, 2, 3, 4, 5, and 6 meters were measured using thermocouples installed in a 5.5-inch hole drilled by an auger. The pipe with the thermocouple was placed vertically in the hole and carefully backfilled and tamped.

4.1. Experimental Framework

Twenty-eight samples were collected and transported to the laboratory for thermal properties testing. The samples were preserved in appropriate containers and stored in suitable conditions until the time of testing. In the laboratory, the samples were categorized, and each category was designated for a specific test. The tests included soil thermal diffusivity, thermal conductivity, and specific heat. The Hot Disk Thermal Constants Analyzer was used to perform these tests on the powder samples. All tests were conducted at the laboratories of Jordan University of Science and Technology.

To ensure accurate and reliable results, the following procedure was established and consistently applied:

- Sample preparation
  - Collect a representative powder sample that accurately represents the soil pile being tested.
  - Select the appropriate sensor for the test. The sensor used is specifically designed for soil or rock powders.
  - Calibrate the testing apparatus by pouring the sample onto the Hot Disk Thermal Constants Analyzer and allowing it to warm up (Figure 11).
- Testing procedure
  - Place the powder sample in the sample holder. The sample holder, made on a lathe, consists of two square parts (10 cm × 10 cm) with a height of 1 cm, as shown in Figure 12.
- Testing Configuration
  - Configure the analyzer software with the appropriate settings
  - Measurement time was 10 second.
  - Power Input: 40 watts.
- Initiate Measurement
  - Results are recorded via the software interface. The Hot Disk sensor applies transient heating power and records the temperature response over time. The analyzer detects the temperature rise in the sample and calculates the corresponding thermal conductivity, thermal diffusivity, and specific heat capacity.
  - Conduct multiple measurements (typically three to five) to ensure reproducibility and accuracy.
  - Reposition the sample or sensor between measurements if necessary to account for any inconsistencies.
- Post-Measurement analysis

The Hot Disk software is configured to analyze and interpret the recorded measurements. The software presents the final findings in its output panel including thermal conductivity, thermal diffusivity, and specific heat capacity based on the transient temperature data and the heat flux equation in its discrete form:

- Compare the results from multiple measurements, considering the contribution of the controlling parameters, assure rationality and consistency.
- Verify the data against known standard or reference materials.
- Repeat the producers for 28 samples.

The soil possesses a variety of characteristics, with thermal conductivity being the most influential factor dictating temperature distribution across the ground. This significant thermal property has been evaluated using the Hot Disk Thermal Constants Analyzer, as shown in Figure 12.

Building samples to cover the Hot Disk sensor from both above and below the frame is part of the process, as shown in Figure 12. The measurement procedure begins by turning on the instrument once the sample has been properly positioned on the sensor surface. The Hot Disk sensor is heated briefly, and the temperature response is recorded. Based on the measured voltage, the device automatically determines the sample's thermal conductivity, thermal diffusivity, and specific heat capacity. This procedure is repeated for each sample, and the results are stored for further assessment and interpretation.

Figure 11. Hot Disk Thermal Constants Analyzer

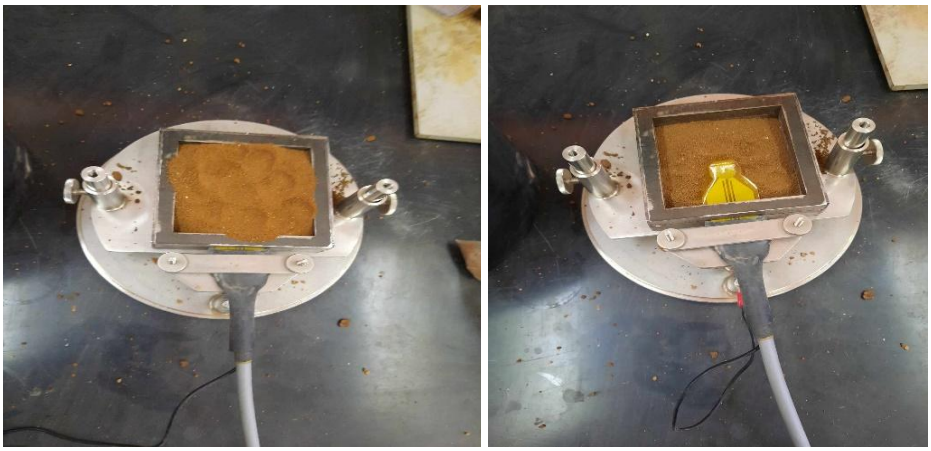

Figure 12. Sample preparation

5. Meteorological Data and Surface Temperature

It is assumed that the boundary condition for solving the mathematical model is the measured near-surface temperature, which was also considered to be uniformly distributed over a large span. This assumption requires that meteorological measurements of the near-surface temperature at the selected locations be made available, which allows for solving the mathematical model. Temperature data were obtained from the Meteorological Department of Jordan [17]. Data screening and refinement were conducted according to the Kaskuda Method. The time variations of temperature across the four seasons (winter, summer, spring, autumn) during the year 2022 are plotted in Figures 1 to 4 above for each season. The variations in temperature over the entire year of 2022 are shown in Figure 13.

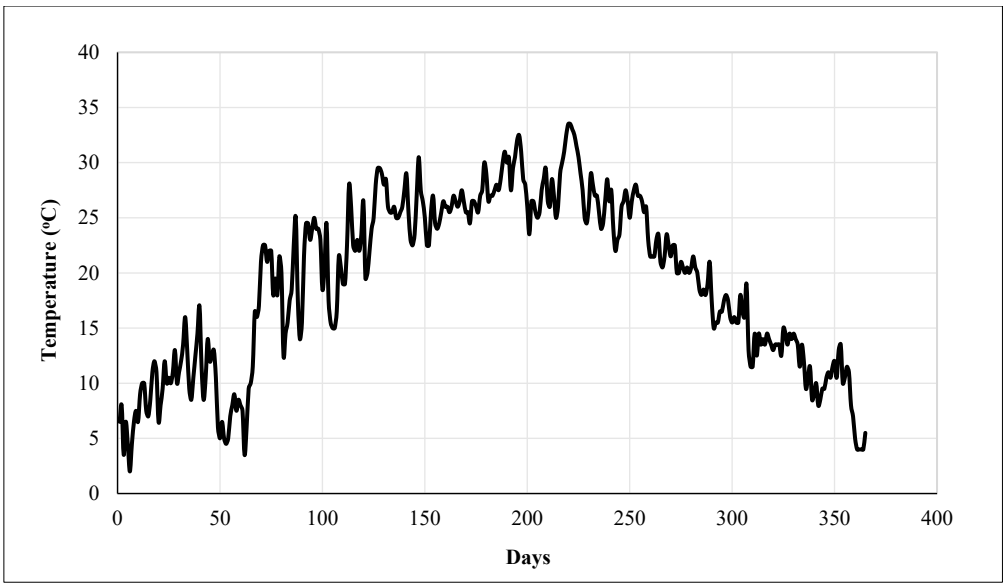

Figure 13. Temperature of 2022 year per day

From Figure 13, it can be observed that the variations can be fairly divided into four seasons, each of which had moderate temperature variations over the length of its time span. This division allows for reasonable averaging of the temperature for each season. The data underwent breakdown, and the temperature cursors were summarized in Table 3. The obtained average temperature is set as the boundary condition for solving the mathematical model.

Table 3. Temperature Summary for the year 2022

	Temperature °C		
	Max.	**Min.**	**Average**
Winter	16	2	10
Spring	30	12	22
Summer	34	24	28
Automn	26	7	18

6. Results and Discussion

The measured values for diffusivity and conductivity are provided in Table 4. The variations with depth are also plotted, as shown in Figures 14 and 15.

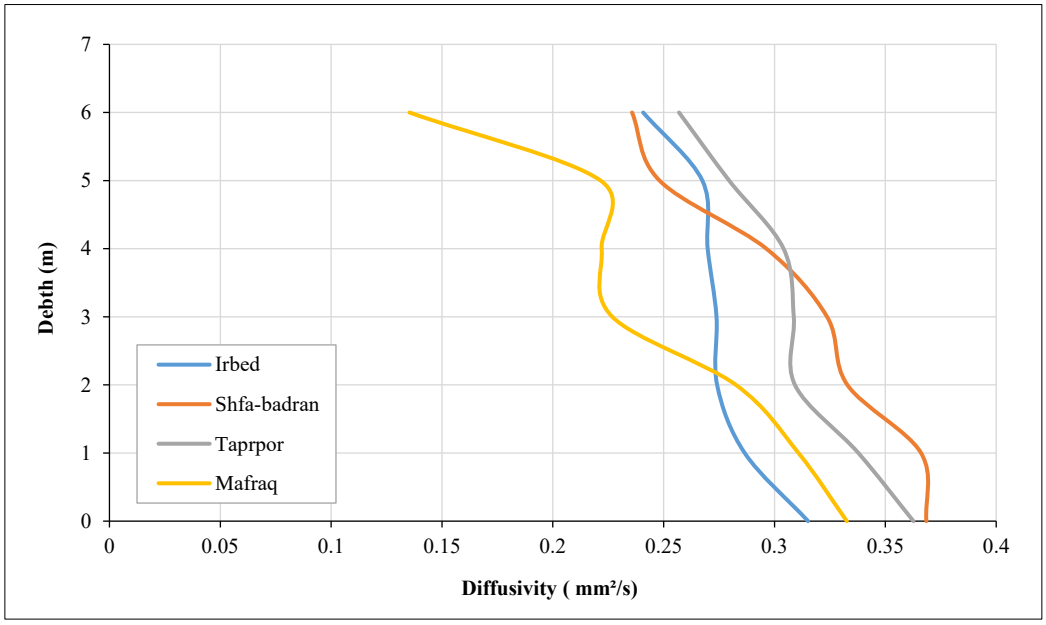

Figure 14. Variations of thermal diffusivity with depth

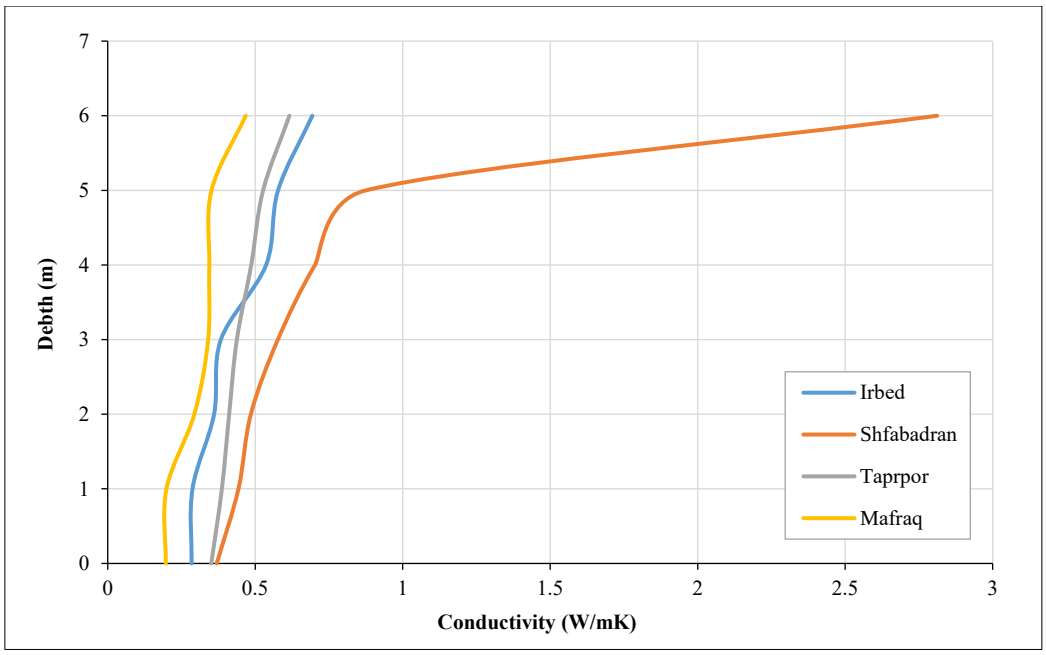

Figure 15. Variations of thermal conductivity with depth

Figures 14 and 15 illustrate the thermal conductivity and thermal diffusivity at the study site locations. The data reveal that as depth increases, thermal diffusivity also increases, while thermal conductivity decreases.

- In Irbid, the thermal conductivity at the surface (0 meters) was 0.315 W/mK, gradually decreasing to 0.24 W/mK. Meanwhile, thermal diffusivity increased from 0.2845 mm²/s to 0.6937 mm²/s.
- In Shafa Badran, the thermal conductivity at 0 meters was 0.368 W/mK, decreasing to 0.248 W/mK. Thermal diffusivity increased from 0.369 mm²/s to 0.875 mm²/s with depth.
- In Tabarbour, the thermal conductivity at 0 meters was 0.362 W/mK, gradually decreasing to 0.256 W/mK. Thermal diffusivity rose from 0.351 mm²/s to 0.616 mm²/s.
- In Mafraq, thermal conductivity at the surface was 0.332 W/mK, declining to 0.135 W/mK, while thermal diffusivity increased from 0.196 mm²/s to 0.467 mm²/s.

These results demonstrate a consistent trend across all locations: thermal conductivity decreases with depth, while thermal diffusivity gradually increases, as shown in Table 4.

Table 4. Variations of thermal diffusivity and conductivity with depth

Z(m)	Irbid		Shafa Badran		Tabarbour		Mafraq	
	Conductivity (W/mK)	Diffusivity (mm²/s)	Conductivity (W/mK)	Diffusivity (mm²/s)	Conductivity (W/mK)	Diffusivity (mm²/s)	Conductivity (W/mK)	Diffusivity (mm²/s)
0	0.3151	0.2845	0.368	0.369	0.362	0.351	0.332	0.196
1	0.2866	0.2875	0.3661	0.443	0.337	0.386	0.310	0.199
2	0.2741	0.3606	0.332	0.485	0.309	0.411	0.282	0.293
3	0.2738	0.3837	0.323	0.576	0.308	0.437	0.226	0.340
4	0.2698	0.5370	0.296	0.702	0.304	0.486	0.222	0.344
5	0.2674	0.5775	0.248	0.875	0.279	0.526	0.221	0.351
6	0.2407	0.6937	0.9	2.87	0.256	0.616	0. 135	0.467

Table 4 presents the thermal conductivity and thermal diffusivity values. For Shafa Badran at a depth of six meters. The results show that the lowest thermal conductivity value is 0.135 W/m·K. while for Mafraq at the same depth, where the temperature amplitude was 1°C. The mean surface temperature, according to the Jordanian climate, was 18°C, and the lowest recorded temperature for the year 2022 was 2°C.

Table 5 summarizes the essential thermal properties of various soil types—namely thermal conductivity, volumetric heat capacity, and thermal diffusivity; as reported by Márquez et al. [18]. These properties play a crucial role in determining the ability of soil to store and transfer heat, which is essential for various applications such as geothermal energy systems, construction, and agricultural planning.

Table 5. Thermal conductivity, volumetric heat, and thermal diffusivity for different kinds of soil [18]

Rock Type	Thermal Conductivity (W/mK)			Volumetric Heat Capacity (MJ/m^{3}K)	Thermal Diffusivity (10^6 m^2/s)		
	Min	Typ	Max		Min	Typ	Max
Basalt	1.3	1.7	2.3	2.6	0.5	0.65	0.88
Greenstone	2	2.6	2.9	2.9	0.69	0.9	1
Gabbro	1.7	1.9	2.5	2.6	0.65	0.73	0.96
Granite	2.1	3.4	4.1	3	0.7	1.13	1.37
Peridotite	3.8	4	5.3	2.7	1.41	1.48	1.96
Gneiss	1.9	2.9	4	2.4	0.79	1.21	1.67
Marble	1.3	2.1	3.1	2	0.65	1.05	1.55
Mica schist	1.5	2	3.1	2.2	0.68	0.91	1.41
Shale sedimentary	1.5	2.1	2.1	2.5	0.6	0.84	0.84
Limestone	2.5	2.8	4	2.4	1.04	1.17	1.67
Loam	1.5	2.1	3.5	2.3	0.65	0.91	1.52
Quartzite	3.6	6	6.6	2.2	1.64	2.73	3
Salt	5.3	5.4	6.4	1.2	4.42	4.5	5.33
Sandstone	1.3	2.3	5.1	2.8	0.46	0.82	1.82
Siltstones and argillites	1.1	2.2	3.5	2.4	0.46	0.92	1.46
Dry gravel	0.4	0.4	0.5	1.6	0.25	0.25	0.31
Water saturated gravel	1.8	1.8	1.8	2.4	0.75	0.75	0.75
Dry sand	0.3	0.4	0.55	1.6	0.19	0.25	0.34
Water saturated sand	1.7	2.4	5	2.9	0.59	0.83	1.72
Dry clay/silt	0.4	0.5	1	1.6	0.25	0.31	0.62
Water saturated clay/silt	0.9	1.7	2.3	3.4	0.26	0.5	0.68
Peat	0.2	0.4	0.7	3.8	0.05	0.1	0.18

By analyzing and comparing the results presented in Table 5, it is evident that the thermal diffusivity of dry gravel is measured at 0.31 mm²/s. This value is remarkably close to the thermal diffusivity recorded for Mafraq, which is 0.467 mm²/s. The similarity between these values can be attributed to the fact that both locations have the same soil type, leading to comparable thermal behavior. Since thermal diffusivity depends on factors such as soil composition, porosity, and moisture content, the close agreement between these values suggests that the gravel in both cases has similar physical characteristics, influencing heat transfer in a comparable manner.

Furthermore, the thermal diffusivity of dry clay, as documented in Table 5, is reported as 0.62 mm²/s. When examining the data from Irbid and Tabarbour, which are two cities known to have the same soil type, it becomes clear that the measured thermal diffusivity at a depth of six meters is 0.69 mm²/s. This value is very close to the numbers presented in Table 1, further reinforcing the consistency of soil thermal properties across different regions that share similar soil compositions. The minor variation in values could be due to slight differences in soil compaction, mineral content, or moisture retention capacity. However, the overall trend confirms that dry clay exhibits relatively low thermal diffusivity compared to other soil types, meaning that heat transfer occurs at a slower rate within such soil structures.

A notable deviation is observed in Shafa Badran, where the measured thermal diffusivity at a depth of five meters is 0.875 mm²/s. As the depth increases to six meters, the thermal diffusivity experiences a significant rise, reaching 1.87 mm²/s. This considerable increase can be attributed to a change in the subsurface composition, as the material transitions from soil to stone. The presence of stone at greater depths significantly alters the thermal properties of the ground, as rocks generally have higher thermal diffusivity compared to soil. This shift highlights the influence of subsurface material variations on thermal behavior, demonstrating how changes in soil composition and depth can significantly affect heat transfer characteristics.

The thermal properties of soil have been compared with those reported in neighboring countries, namely Saudi Arabia (references) and Iraq (references), as well as with some typical benchmark values (references). In this study, the thermal conductivity ranges from 0.2407 to 0.368 W/m·K (excluding anomalies), with an average value of 0.315 W/m·K. In Iraq, according to Jahanger (2021), thermal conductivity varies from as low as 1.1 to as high as 1.8 W/m·K.

In Saudi Arabia, studies conducted on Hijaz soils by Sharqawy et al. (2009) report thermal conductivity values ranging from 0.154 to 0.271 W/m·K, with an average of 0.207 W/m·K [19, 20].

In conclusion, the comparison of thermal diffusivity values across different soil types and locations illustrates the importance of soil composition, depth, and material transitions in influencing thermal properties. The findings confirm that regions with similar soil types tend to exhibit comparable thermal diffusivity values, whereas locations experiencing shifts in ground composition, such as in Shafa Badran, display notable variations in heat transfer properties. Understanding these variations is essential for optimizing the design and efficiency of thermal energy storage, geothermal systems, and construction projects that depend on stable soil thermal properties.

The ground temperature variations measured in boreholes using the thermocouples are provided in Table 6. The Table shows that there is a slight temperature difference at depths of 5 meters and below. Temperature variations over 14 days at a depth of 6 meters are shown in Figure 16. The findings indicate that ground temperature remains relatively stable throughout the year at depths of 5 meters and below, ranging between 14 and 16 °C. However, there is a slight variance of approximately 3 °C. The temperature variations—both predicted and measured—at a depth of 6 meters are plotted against time in Figure 17, showing a reasonably stable temperature profile. The predicted values are consistently about 3 °C higher than the measured values on average. There is a slight temperature difference at a depth of 5 meters or less; however, the temperature remains nearly the same and can be used in many applications.

Table 6. Measured versus predicted value of temperature profile

Depth (m)	1		2		3		4		5		6	
Day	Measured	Predicted	Measured	Predicted	Measured	Predicted	Measured	Predicted	Measured	Predicted	Measured	Predicted
15-Mar	29	25.5	25.5	25.5	21	25	17	19	16	18	14	18
14-Mar	31	25.5	25.5	25.5	20	25	16	19	16	18	14	18
13-Mar	30	26	26	26	20	25	15	19	16	18	14	18
12-Mar	23	25	25	25	21	25	16	19	16	18	١٥	18
11-Mar	29	25	25	25	21	25	15	19	16	18	15	18
10-Mar	27	25.5	25.5	25.5	20	25	16	19	15	18	14	18
9-Mar	26	26	26	26	19	25	15	19	15	18	14	18
8-Mar	30	27.5	27.5	27.5	23	25	16	19	16	18	15	18
7-Mar	26	29	29	29	21	25	16	19	16	18	16	18
6-Mar	29	25.5	25.5	25.5	21	25	17	19	15	18	15	18
5-Mar	27	23	23	23	21	25	15	19	16	18	14	18
4-Mar	28	25.5	25.5	25.5	23	25	17	19	16	18	15	18

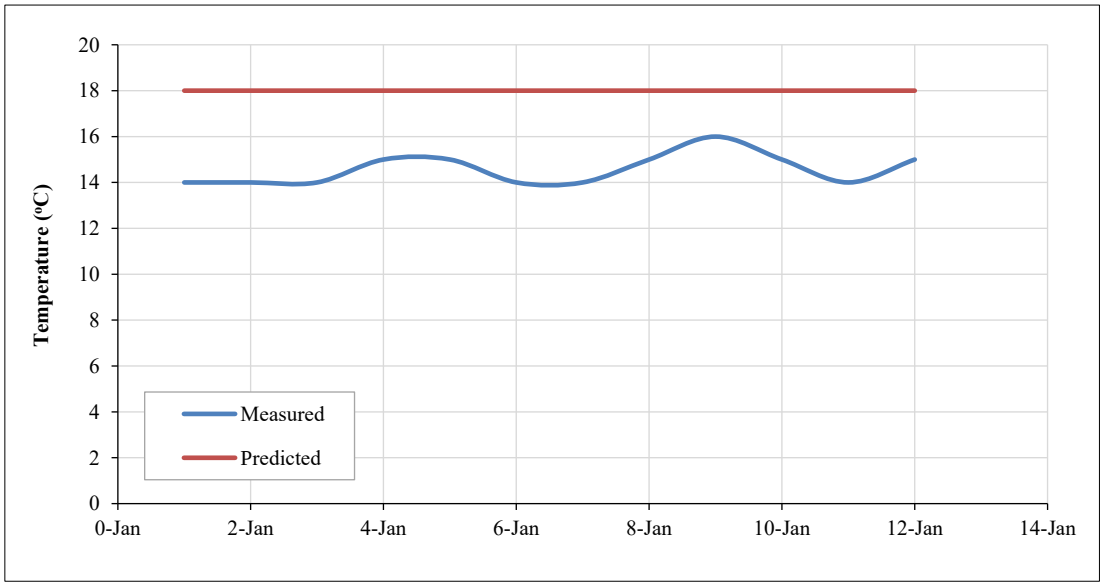

Figure 16. Measured and predicted temperature at depth of 6 meter

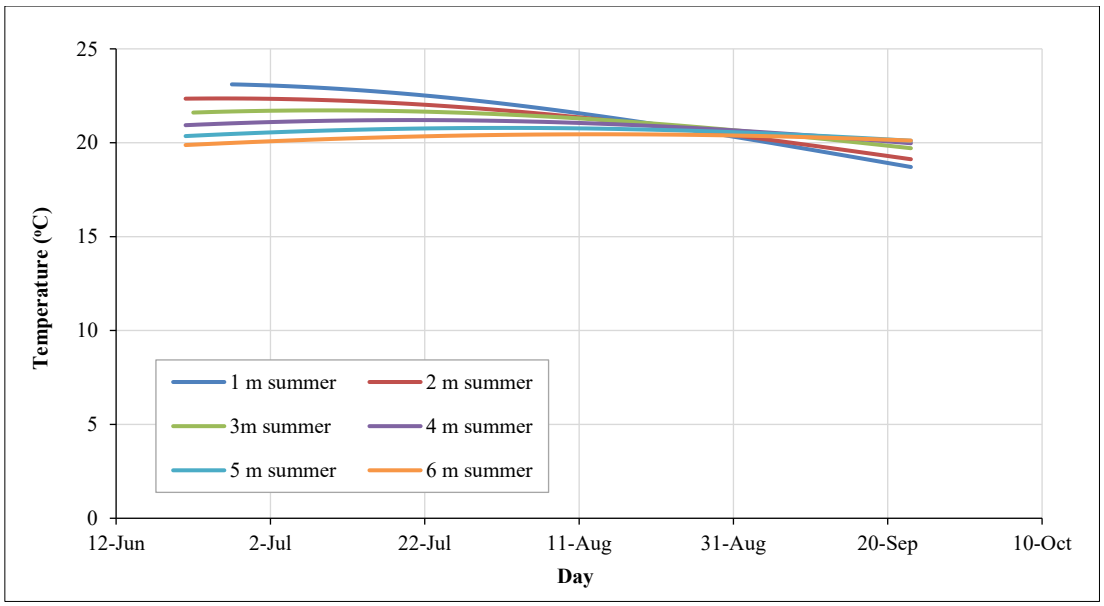

Figure 17. Temperature gradient of summer season

Equation 2 demonstrates how the thermal inertia of the soil causes the amplitude of thermal fluctuations to decrease steadily with increasing depth, gradually eliminating the maximum and minimum values. The phase transition is reached within two months at a depth of five meters. Deeper depths experience less annual variation, gradually approaching the site's average annual temperature. Under realistic conditions, soil temperature changes occur between the surface and approximately 3 meters below due to factors such as soil type, compaction, homogeneity, moisture, and groundwater, all of which influence geothermal diffusion. Consequently, the actual temperature curves may not exhibit the uniform distribution shown in Figure 18—an aspect often overlooked when analyzing geothermal diffusion from streams, where temperatures are typically considered constant. By dividing the climate into four seasons, we can reduce the margin of error and obtain temperatures with more reasonable fluctuations. Accordingly, Figures 18 to 20 illustrate the temperatures in the Earth's interior over the four seasons of 2022.

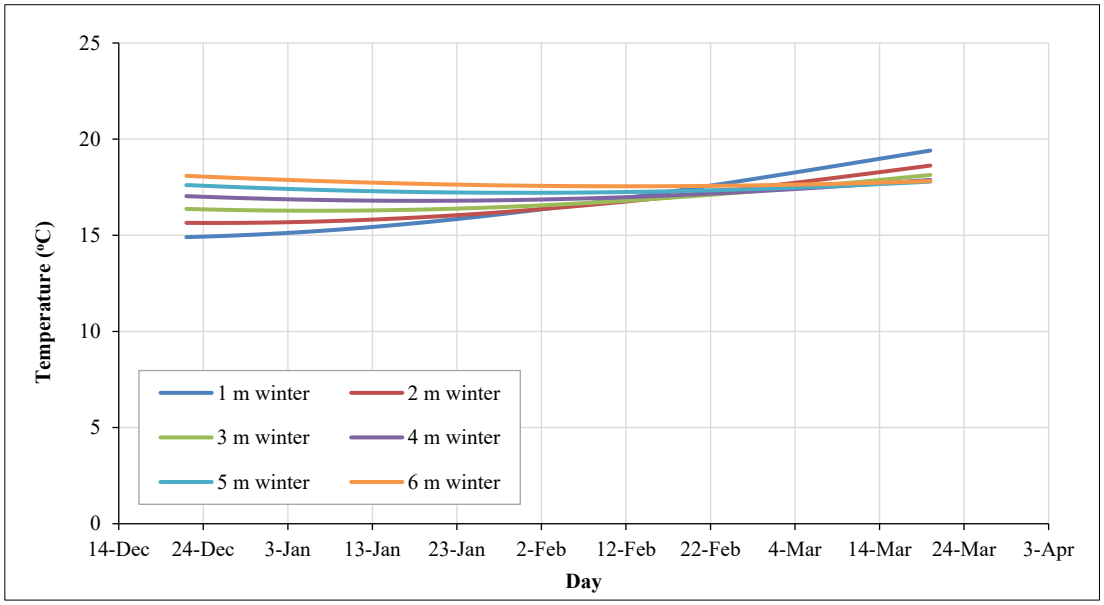

Figure 18. Temperature gradient of winter season

Figures 16 to 20 show that as depth increases, the amplitude of thermal fluctuations decreases, and the maximum and minimum values gradually diminish due to the thermal inertia of the soil itself. At a depth of 5-6 meters, the metamorphic phase reaches an almost steady state. As the depth increases, annual soil temperature fluctuations decrease, and temperatures tend to fall, approaching the annual average. In practice, at depths ranging from the surface to about 10 meters, the soil temperature varies. This indicates that the spread of geothermal energy will not be constant. Temperature variations, as predicted by the mathematical model, are shown in Figure 21.

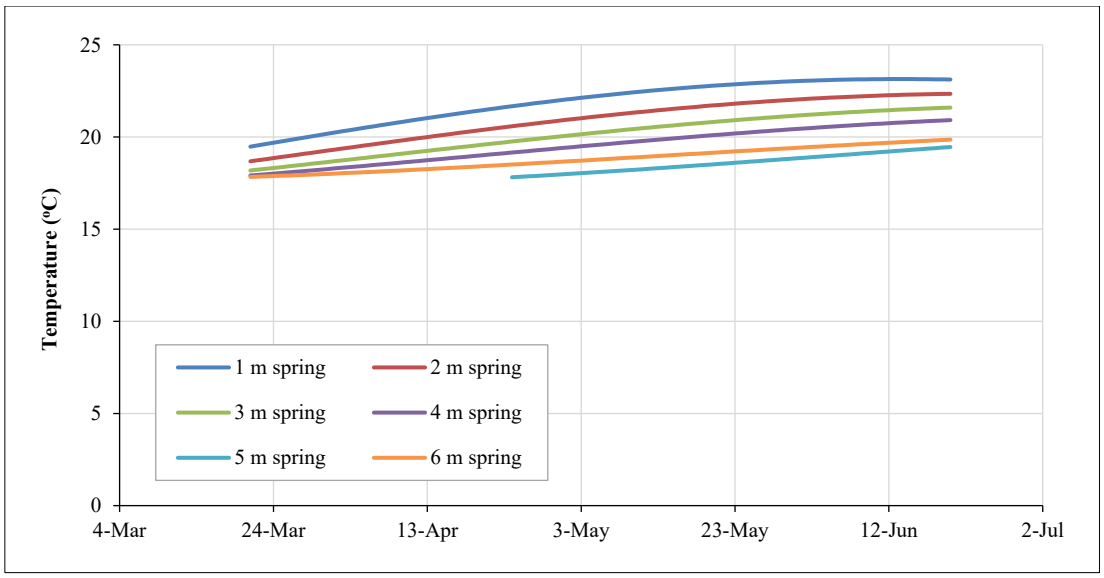

Figure 19. Temperature gradient of spring season

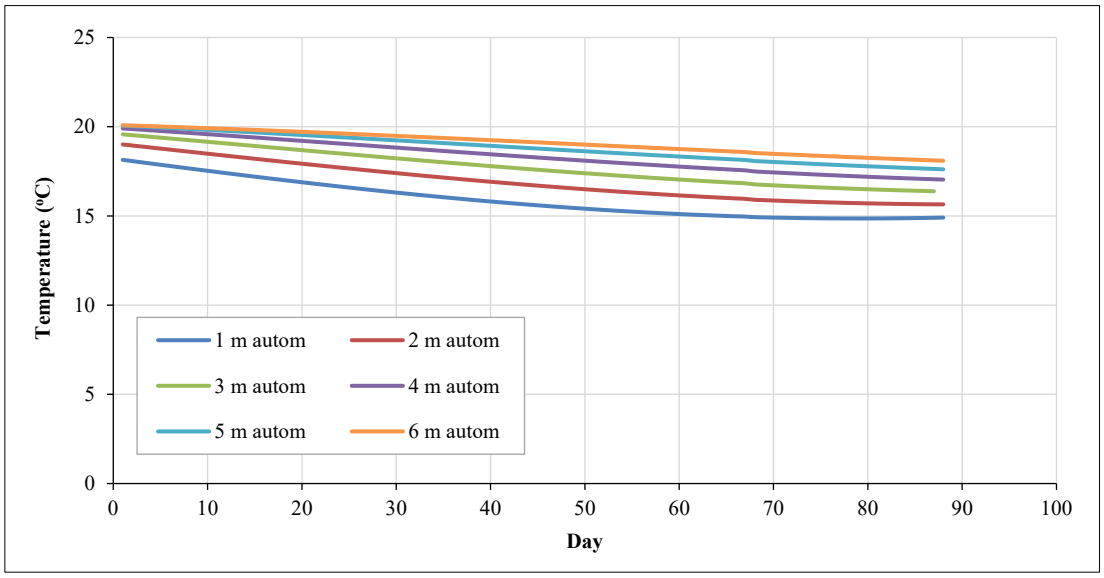

Figure 20. Temperature gradient for the fall season

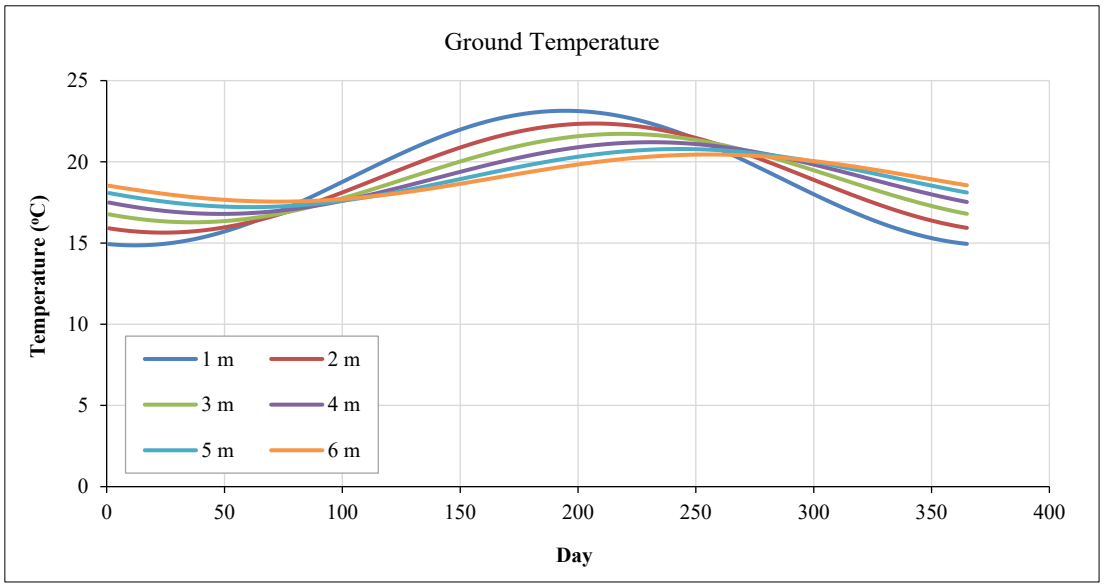

Figure 21. Typical temperature behavior of the soil close to the surface at different depths. The curves show the evolution of the temperature from the surface 0 m to 6 m depth

7. Discussion

The resulting ranges of diffusivity, conductivity, heat capacity, and specific heat fall within the category of materials with a high capacity to absorb, store, and conduct heat. This positions these materials as having strong potential for producing or absorbing heat energy in various applications. Furthermore, the relatively constant temperature profile observed below 5 to 6 meters indicates the potential for utilizing ground energy at both shallow depths (less than 5 meters, due to favorable thermal properties) and deeper levels (greater than 6 meters, due to the temperature stability).

Figures 1 to 4 and Figure 13 demonstrate that surface temperature differs significantly from ground temperature. According to Figures 17 to 20, this difference is particularly pronounced in winter and summer, indicating a relatively high heat transfer gradient. This suggests that when a fluid—such as air, water, or oil—is circulated through the soil, it can effectively absorb or release heat, provided that the heat transfer occurs within reasonable limits of time and quantity, as informed by the conductivity and diffusivity values listed in Table 4.

The variations in diffusivity, shown in Figure 14, range from slightly less than 0.15 mm^2/s to slightly more than 0.35 mm^2/s. These values are consistent with the expected material properties and can be calculated according to IEC 60853-2. Diffusivity clearly increases with depth. Given that the soil profile and geologic formation are reasonably uniform, this variation is likely due to pressure increases resulting from the weight of the overlying soil or rock column, and the resulting increase in density at greater depths due to natural geo-compaction, which lowers the void ratio.

Regarding thermal conductivity (Figure 15 and Table 4), values range from approximately 0.2 W/m·K near the surface to 0.9 W/m·K at a depth of 6 meters. Conductivity increases with depth, which aligns with the inverse relationship to resistivity and the associated increases in pressure and density. This implies that mineral particles in deeper soil layers are more closely packed, reducing the void ratio and shortening the thermal path, thereby improving heat transfer efficiency. The differences observed between the curves in Figures 14 (diffusivity) and 15 (conductivity), and the values listed in Table 5 can be primarily attributed to differences in soil mineral composition across locations. This is because the other major influencing factors—such as water content and void ratio—did not differ significantly between the four sites to account for the observed variations.

The measured soil properties were incorporated into a mathematical model to calculate temperature variations across the soil/rock profile. The resulting temperature distribution, based on both the model and measured properties, was compared with the actual measured temperature profile. The two were in close agreement, as shown in Figures 15 to 20.

8. Conclusion

This research lays the foundation for the study and utilization of geothermal energy in Jordan. The results of thermal diffusivity and heat conductivity tests, along with the measured ground temperature profile, have been confirmed to be promising for shallow geothermal applications. These findings consistently fall within the range of ground thermal properties observed in regions where geothermal energy projects have been successfully implemented. The four key regions investigated in this study represent both the primary geographic areas and the common soil types found across Jordan. They also encompass the country's diverse climate zones. All findings and associated data indicate a strong potential for the efficient use of ground thermal energy. Further research involving greater depths, additional influencing parameters, broader applications, and pilot testing should be conducted to determine the most effective methods and uses. Mathematical modeling and comparisons with other regions have supported these implications. The typical annual average temperature in Jordan is 18°C, with the lowest recorded temperature reaching 2°C in 2022. The lowest thermal diffusivity value recorded was 0.135, observed when the temperature amplitude was 1°C. Correspondingly, the soil's thermal inertia reduces temperature fluctuation amplitudes with depth, leading to a two-month phase shift at a depth of five meters. In practical scenarios, variables such as soil type and moisture content introduce variations in soil temperature, challenging the common assumption that thermal diffusivity remains constant.

9. Declarations

9.1. Author Contributions

Conceptualization, M.I., S.Q., and W.A.B.; methodology, M.I., S.Q., and W.A.B.; validation, M.I., S.Q., and W.A.B.; formal analysis, S.Q.; investigation, S.Q.; resources, M.I.; data curation, S.Q.; writing—original draft preparation, S.Q.; writing—review and editing, W.A.B.; visualization, S.Q.; supervision, M.I. and W.A.B.; project administration, M.I. All authors have read and agreed to the published version of the manuscript.

9.2. Data Availability Statement

The data presented in this study are available on reasonable request from the corresponding author.

9.3. Funding

The authors received no financial support for the research, authorship, and/or publication of this article.

9.4. Conflicts of Interest

The authors declare no conflict of interest.

10. References

[1] Buzăianu, A., Csáki, I., Moţoiu, P., Popescu, G., Thorbjornsson, I., Ragnarsodottir, K. R., Guðlaugsson, S., & Goubmunson, D. (2015). Recent Advances of the Basic Concepts in Geothermal Turbines of Low and High Enthalpy. Advanced Materials Research, 1114, 233–238. doi:10.4028/www.scientific.net/amr.1114.233.

[2] Vettkrlein, E. (1973). Taylor, S.A., and Ashcroft, G. L., The Physics of Irrigated and Nonirrigated Soils. Pedobiologia, 13(6), 457–458. doi:10.1016/s0031-4056(23)02134-0.

[3] International Renewable Energy Agency (IRENA). (2011). Renewable Readiness Assessment: The Hashemite Kingdom of Jordan. International Renewable Energy Agency (IRENA), Masdar City, United Arab Emirates. Available online: https://moenv.gov.jo/ebv4.0/root_storage/en/eb_list_page/irena_rra_jordan_2021.pdf (accessed on July 2025).

[4] Jia, G. S., Tao, Z. Y., Meng, X. Z., Ma, C. F., Chai, J. C., & Jin, L. W. (2019). Review of effective thermal conductivity models of rock-soil for geothermal energy applications. Geothermics, 77, 1–11. doi:10.1016/j.geothermics.2018.08.001.

[5] Abu-Hamdeh, N. H. (2000). Effect of tillage treatments on soil thermal conductivity for some Jordanian clay loam and loam soils. Soil and Tillage Research, 56(3–4), 145–151. doi:10.1016/S0167-1987(00)00129-X.

[6] Yusof, T. M., Anuar, S., & Ibrahim, H. (2014). Numerical investigation of ground cooling potential for Malaysian climate. International Journal of Automotive and Mechanical Engineering, 10(1), 2081–2090. doi:10.15282/ijame.10.2014.24.0175.

[7] Cao, D., Shi, B., Loheide, S. P., Gong, X., Zhu, H. H., Wei, G., & Yang, L. (2018). Investigation of the influence of soil moisture on thermal response tests using active distributed temperature sensing (A–DTS) technology. Energy and Buildings, 173, 239–251. doi:10.1016/j.enbuild.2018.01.022.

[8] García-Noval, C., Álvarez, R., García-Cortés, S., García, C., Alberquilla, F., & Ordóñez, A. (2024). Definition of a thermal conductivity map for geothermal purposes. Geothermal Energy, 12(1). doi:10.1186/s40517-024-00292-8.

[9] Stemmle, R., Lee, H., Blum, P., & Menberg, K. (2023). City-scale heating and cooling with Aquifer Thermal Energy Storage (ATES). Hydrology and Earth System Sciences, 1-27. doi:10.5194/hess-2023-62.

[10] Ouerghi, F. H., Omri, M., Nisar, K. S., Abd El-Aziz, R. M., & Taloba, A. I. (2024). Investigating the potential of geothermal energy as a sustainable replacement for fossil fuels in commercial buildings. Alexandria Engineering Journal, 97, 215–229. doi:10.1016/j.aej.2024.03.094.

[11] Kerme, E. D., Alzahrani, W. S., Fung, A. S., & Leong, W. H. (2024). Experimental investigation of ground-source heat pump system coupled to vertical and horizontal ground loops: A case study. Renewable Energy, 236, 121482. doi:10.1016/j.renene.2024.121482.

[12] Haj Assad, M. E., Nooman AlMallahi, M., Ramadan, A., Awad, M. A., Rejeb, O., & AlShabi, M. (2022). Geothermal Heat Pumps: Principles and Applications. 2022 Advances in Science and Engineering Technology International Conferences (ASET), 1–8. doi:10.1109/aset53988.2022.9734907.

[13] Penrod, E. B., Walton, W. W., & Terrell, D. V. (1958). A Method to Describe Soil Temperature Variation. Journal of the Soil Mechanics and Foundations Division, 84(1). doi:10.1061/jsfeaq.0000098.

[14] Carson, J. E. (1963). Analysis of soil and air temperatures by Fourier techniques. Journal of Geophysical Research, 68(8), 2217–2232. doi:10.1029/jz068i008p02217.

[15] Larwa, B. (2019). Heat transfer model to predict temperature distribution in the ground. Energies, 12(1), 25. doi:10.3390/en12010025.

[16] Carslaw, H.S. & Jaeger, J.C. (1959) Conduction of Heat in Solids (2nd Ed.). Oxford University Press, New York, United States.

[17] JMD. (2025). Department of Meteorology, Jordan Meteorological Department, Amman, Jordan. Available online: https://jmd.gov.jo/en (accessed on July 2025).

[18] Márquez, J. M. A., Bohórquez, M. Á. M., & Melgar, S. G. (2016). Ground thermal diffusivity calculation by direct soil temperature measurement. application to very low enthalpy geothermal energy systems. Sensors (Switzerland), 16(3), 306. doi:10.3390/s16030306.

[19] Jahanger, Z. K. (2021). Evaluation of the thermal conductivity of middle part of Iraqi soil. Materials Today: Proceedings, 42, 2431–2435. doi:10.1016/j.matpr.2020.12.553.

[20] Sharqawy, M. H., Said, S. A., Mokheimer, E. M., Habib, M. A., Badr, H. M., & Al-Shayea, N. A. (2009). First in situ determination of the ground thermal conductivity for borehole heat exchanger applications in Saudi Arabia. Renewable Energy, 34(10), 2218–2223. doi:10.1016/j.renene.2009.03.003.